Numerical analysis of impact breakage in caving mining

Á. Vergara[a], R. Fuentes[a] and S. Palma[b]
[a]*RWTH Aachen, Aachen, Germany*
[b]*Universidad Técnica Federico Santa María, Santiago, Chile*

ABSTRACT

This work investigates the fracture characteristics of a rock system subject to impact in caving mining through the direct application of the Fast-Breakage Model (FBM), validated with experimental impact tests. The study focuses on the transition stage between primary and secondary fragmentation in caving mining, allowing the characteristics and breakage probability post-impact to be investigated under various conditions. The results show a strong influence of both the size ratio and the height of the air gap on the fragmentation of the system, increasing the breakage probability of the rock blocks and inducing the formation of fines. These findings seek to contribute to the control of caving to optimise the degree of fragmentation obtained at the drawpoint and reduce the geomechanical risks implied by the dynamic change of the stress system within the rock mass.

1 INTRODUCTION

Block caving has been characterised as a viable and highly productive underground mining method for the exploitation of massive orebodies. The method applied massively in much of the world, is not exempt from the complexities involved in the geomechanical treatment of the rock mass. Considering the gradual migration of orebodies operated by open pits towards underground methods, block caving has taken on greater relevance within applied geomechanics. Various factors have been identified as the main sources of interest in the implementation of the method. Caveability, fragmentation, layout, induced cave stresses, exploitation sequencing, dilution, subsidence and draw extraction are some critical parameters that must be well known in the design of a caving mining project (Laubscher, 1994).

The rock mass fragmentation process during caving is characterised by the presence of three well-defined stages: (1) in-situ fragmentation, defined as the natural state of the network of discontinuities within the rock mass; (2) primary fragmentation, defined by the size of the rock blocks formed in the cave back once the tensional state of the orebody has been altered, and (3) secondary fragmentation, characterised by the wear and attrition of rock fragments in the mineral column, as they descend towards the drawpoints (Brown, 2002). However, a brief transition stage can be described between primary and secondary fragmentation, where the primary blocks detach from the cave back, impacting the mineral column. This stage, characterised mainly by an impact fracture, has been ignored in the different fragmentation analyses of the rock mass.

Various approaches have been applied to evaluate or predict the degrees of fragmentation in caving. Empirical and numerical methods based on experience (Esterhuizen, 2005; Laubscher & Jakubec, 2001), experimental tests (Castro et al., 2014; Dorador et al., 2014; Gómez & Castro, 2022), and attractive semi-empirical approaches (Gómez et al., 2017; Pierce et al., 2010; Veltin et al., 2021) have been part of some proposals to predict rock mass fragmentation.

The main objective of this work is to present a novel numerical approach to complement and characterise the impact breakage of rock blocks, to determine both the breakage probability and the characteristics of fragmentation. The idea is to propose a starting point for the analysis of fragmentation considering the rock impact processes, where we hypothesise that secondary fragmentation occurs at the moment the primary rock hits the caved ore, inducing a degree of initial fragmentation.

2 NUMERICAL SCHEME

2.1 Fast-Breakage modelling in a discrete framework

The numerical fracture mechanism implemented in the discrete-element framework used in this work is based on the statistical fracture model proposed by Vogel & Peukert (2004) and validated and expanded by Shi & Kojovic (2007), which allows describing the fracture through similarity reasoning (Rumpf, 1973) and the Weibullian behaviour of the fracture mechanics (Weibull, 1951). This model allows the instantaneous breakage of each particle based on the amount of energy it receives. The degree of fragmentation is determined by the breakage probability $P(E)$ of the particle of size d_i as a function of the cumulative specific impact energy received in each stressing event:

$$P(E) = 1 - \exp\left[-SE\left(\frac{d_i}{d_{ref}}\right)\right] \tag{1}$$

and

$$E_{min} = E_{min,ref}\left(d_{ref}/d_i\right) \tag{2}$$

where S is a measure of the resistance to fracture of the material, E the cumulative specific impact energy by the particle prior to each stressing event, E_{min} the minimum energy supported by the particle under which it does not experience breakage and d_{ref} a reference particle size (usually based on existing experimental calibration).

Once the particle reaches its resistance threshold ($E > E_{min}$), it breaks, and the degree of fragmentation is calculated based on the incomplete beta function (family of t_n-curves).

$$t_n = \frac{100}{\int_0^1 x^{\alpha_n - 1}(1-x)^{\beta_n - 1}\,dx}\int_0^{t_{10}} x^{\alpha_n - 1}(1-x)^{\beta_n - 1}\,dx \tag{3}$$

and

$$t_{10} = A\left\{1 - \exp\left[-SE\left(\frac{d_i}{d_{ref}}\right)\right]\right\} \tag{4}$$

where t_{10} is the fineness index (equivalent to the percentage of material that passes through the screen one tenth of the initial size), A is the maximum t_{10} value (based on material calibration) and α_n and β_n are the coefficients of the function, that must to be fit to the experimental data of the t_n-t_{10} curve (Table 2). The fracture of the rock material allows the generation of progeny fragments according to the Laguerre-Voronoi tessellation algorithm (Imai et al., 1985). This is based on the generation of generator points in space (centroids of the progeny fragments), concentrated in a close vicinity to the point of contact, so the fracture is represented with finer fragments at the point of contact, and thicker far from such vicinity.

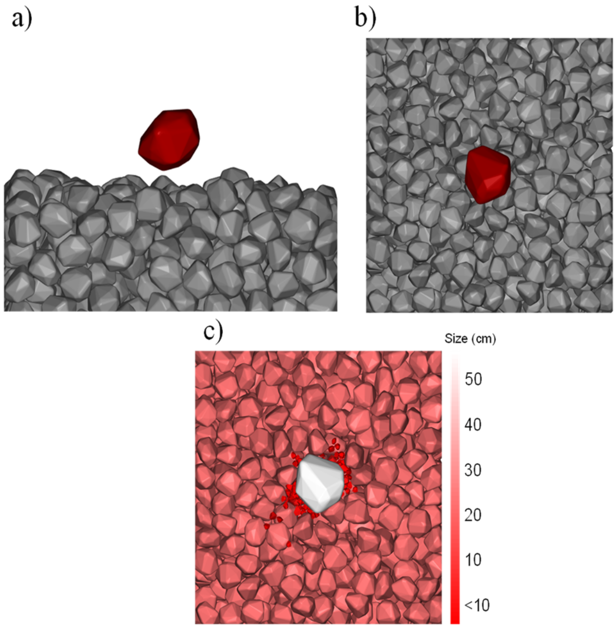

Figure 1 Model configuration. (a) front view at $t = 0$; (b) top view at $t = 0$, and (c) top view at $t > t_{imp}$.

2.2 Model setup

The system consists of a monodisperse rock bed (caved ore) on which the rock block (primary rock) impacts. Figure 1 shown below, represents the main scheme of the system to be modelled. The geometry of the rock system is irregular-shaped, both to more realistically represent the shape of the rock, as well as the dynamics of the fracture of brittle materials. Table 1 shows the characteristic sizes of the rocks and the different air gap heights considered in the simulation.

Table 1 Geometric parameters applied in the study

Parameter	Values (m)
Primary block size, D	[0.1, 0.2, 0.4, 1, 2]
Caved ore size, d	0.2
Air gap height, h	[1, 5, 10, 20]
Reference size, d_{ref}	0.005

At the simulation time $t = 0$, the caved ore is gravitationally deposited as a rock layer, the primary block is placed on the caved ore and an initial impact velocity v_{imp} is applied. This velocity is obtained from mechanical energy conservation, based on the height of the air gap $v_{imp} = \sqrt{2gh}$.

Table 2 Material breakage parameters (low-grade copper ore) used in the simulations

Density (kg/m^3)	2930
Elastic Modulus (GPa)	52
Poisson's ratio	0.25
Friction Coef.	0.38
Specific energy (J/kg)	100
Selection function (kg/J)	0.002
Maximum t_{10}	0.67
Incomplete beta function coefficients	
$\alpha_{1.2}/\beta_{1.2}$	0.51/11.95
$\alpha_{1.5}/\beta_{1.5}$	1.07/13.87
α_2/β_2	1.01/8.09
α_4/β_4	1.08/3.03
α_{25}/β_{25}	1.01/0.53
α_{50}/β_{50}	1.03/0.36
α_{75}/β_{75}	1.03/0.30

The rock material is modelled as a low-grade copper ore and its properties are shown in Table 2. The main mechanical parameters of the material were obtained by calibrating the numerical model with the impact tests carried out by Barrios et al. (2020) and Jiménez-Herrera et al. (2018). The results of the calibration are presented in Figure 2.

To simplify the analysis, two dimensionless variables have been considered that reduce and facilitate the presentation of the results: the size ratio $D^* = D / d$ and the normalised impact velocity $v^* = v^2/gD$. This impact ratio encompasses both the effects of impact velocity v and rock block size D. Thus, based on Table 1, the size ratio D^* fluctuates between the values [0.5-10], while the impact ratio fluctuates between [0-500].

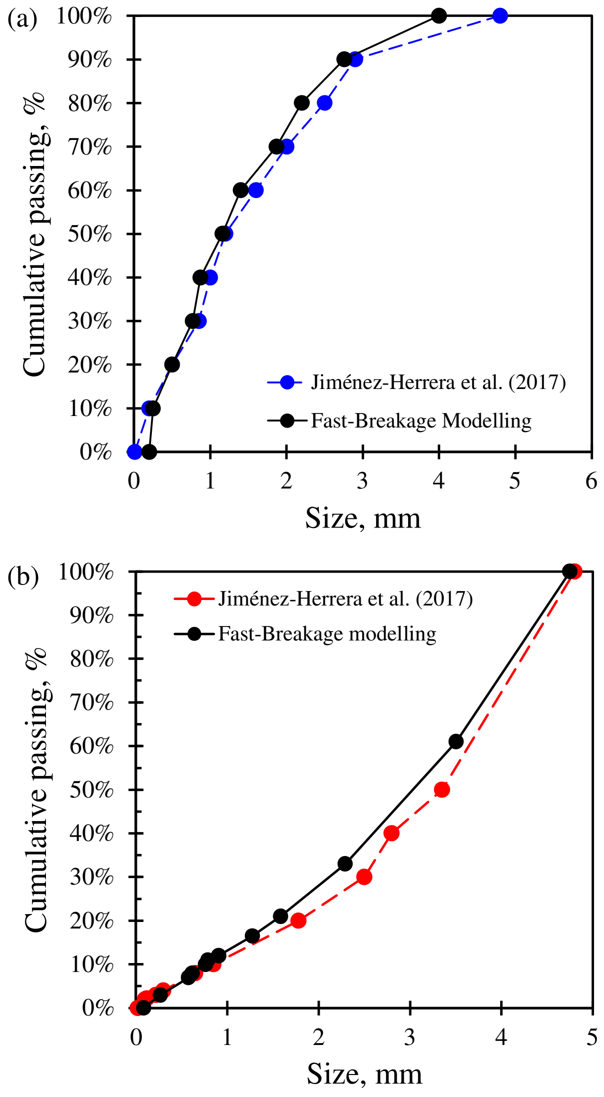

Figure 2 Calibration using impact tests: (a) single particle and (b) multiple particles.

3 RESULTS AND DISCUSSION

The results below summarise the effects of the air gap and the rock block size on breakage probability behaviour. We can understand this breakage probability of the rock block as the survival rate that the rock experiences under different conditions. Figure 3 shows the influence of the air gap on the breakage probability of both the rock block and the caved ore, for different size ratios.

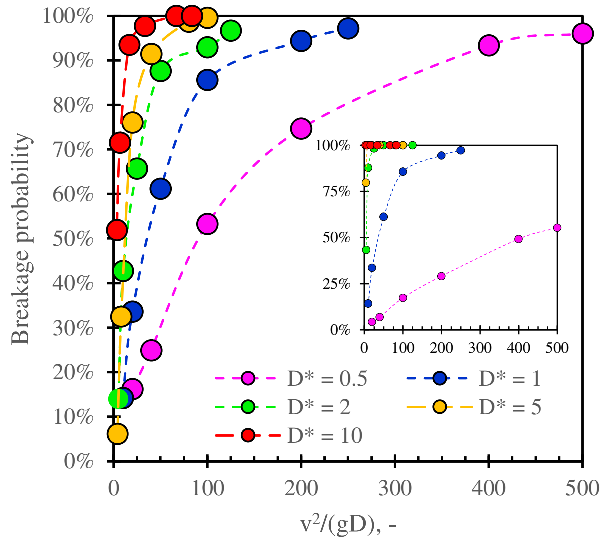

Figure 3 **Breakage probability of the rock block and the caved ore (inside) as a function of the normalised velocity.**

This expected behaviour shows that the greater the air gap, the greater the specific potential energy (energy per unit mass) that the rock block stores prior to its fall, which results in a greater probability of its fracture.

On the other hand, when the size ratio increases, the breakage probability of the rock block increases, mainly due to the size effect, where larger rocks are more prone to fracture compared to smaller ones. As can be seen in the plot, there is a point where the caved ore experiences fracture practically independent of the impact energy ($D^* > 1$), but rather in the size ratio compared to the rock block.

Figure 4 shows the contact force chains of the system at impact. This network allows determining the area of dynamic influence of the impact. Considering that the granular medium is highly dissipative, the caved ore stores the impact energy in the form of deformation energy, which allows the accumulation of energy prior to fracture (until it reaches its maximum strength). Therefore, this type of scheme helps with the determination of dynamic influence on the mineral column (e.g. in a hang-up, where large primary blocks fall onto the mineral column). However, this network of forces gradually disappears as the rock block penetrates the caved ore.

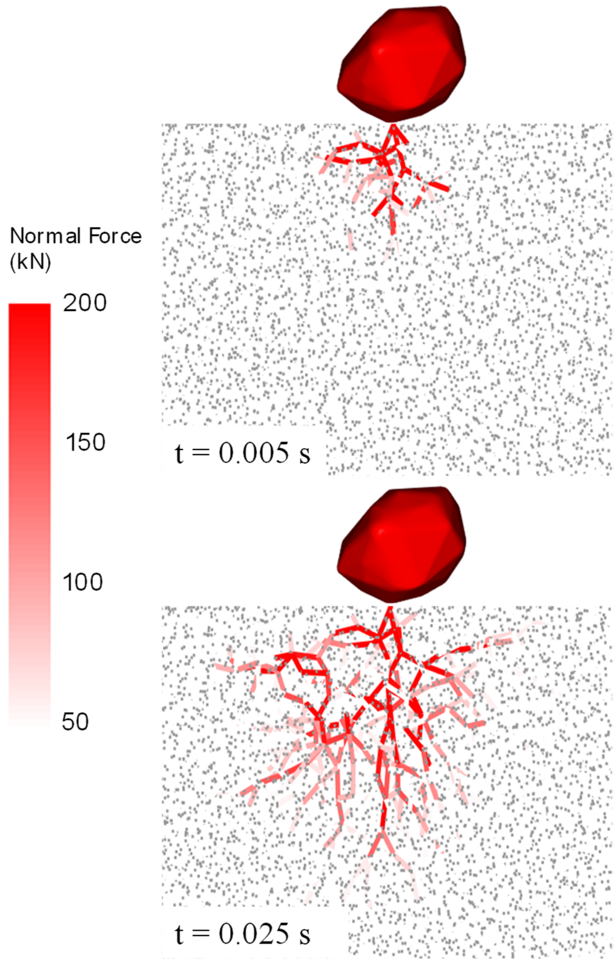

Figure 4 **Contact force chains inside the caved ore during the impact.**

With respect to the size distribution, Figure 5 presents the family of particle size distribution curves for different block sizes, with an impact height of 10 m. It is important to highlight the pattern of similarity between the curves, showing that rocks of the same material have a similar fracture pattern, for similar impact conditions (in this case, $h = 10$ m).

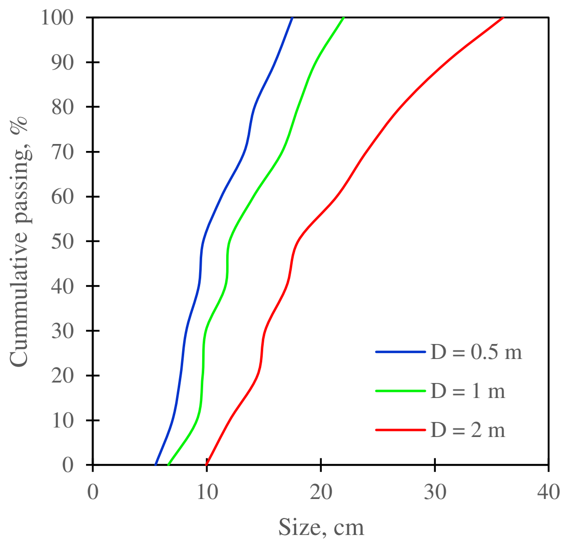

Figure 5 Fragment size distribution of the rock block after impact, for different block sizes.

4 CONCLUSIONS

Numerical modelling using discrete-element techniques of impact breakage of rocks has been carried out to analyse the general dynamics of the rock fragmentation process in caving mining, applied to the transition stage between primary and secondary fragmentation.

The breakage probability of the rock block is greater as its size increases. Furthermore, this probability also increases when the impact energy that the block receives is greater. This probability is very well described based on the Weibullian behaviour of the fracture process, extending this statistical proposal to the analysis of impact fracture of rock systems.

Through the force network scheme, it is possible to determine the unstable area during the impact, allowing its influence on the different levels of the mine to be predicted.

The fracture model also allows a description of the size distribution of fragments, which aids to predict and estimate the behaviour of the size pattern after the impact, and which directly affects the control and/or mitigation of the system in which it is involved.

The results of this work allow a great approach to the computational modelling of the fracture process in rock media, as an alternative to the evaluation of the degree of fragmentation of granular systems subjected to impact.

REFERENCES

Barrios, G. K. P., Jiménez-Herrera, N. & Tavares, L. M. (2020). Simulation of particle bed breakage by slow compression and impact using a DEM particle replacement model. *Advanced Powder Technology*, *31*(7), 2749–2758. https://doi.org/10.1016/j.apt.2020.05.011

Brown, E. T. (2002). Block Caving Geomechanics: International Caving Study 1997-2000. Julius Kruttschnitt Mineral Research Centre, The University of Queensland.

Castro, R. L., Fuenzalida, M. A. & Lund, F. (2014). Experimental study of gravity flow under confined conditions. *International Journal of Rock Mechanics and Mining Sciences*, *67*, 164–169. https://doi.org/10.1016/j.ijrmms.2014.01.013

Dorador, L., Eberhardt, E., Elmo, D. & Aguayo, A. (2014). Influence of secondary fragmentation and column height on block size distribution and fines migration reaching drawpoints. 3rd International Symposium on Block and Sublevel Caving. https://www.researchgate.net/publication/263199359

Esterhuizen, G. (2005). A program to predict block cave fragmentation. Technical reference and Users Guide (3.05).

Gómez, R. & Castro, R. (2022). Experimental Quantification of Granular Material Fragmentation Due to Travel Distance. *Mining, Metallurgy and Exploration*, *39*(2), 615–623. https://doi.org/10.1007/s42461-022-00545-9

Gómez, R., Castro, R. L., Casali, A., Palma, S. & Hekmat, A. (2017). A Comminution Model for Secondary Fragmentation Assessment for Block Caving. *Rock Mechanics and Rock Engineering*, *50*(11), 3073–3084. https://doi.org/10.1007/s00603-017-1267-2

Imai, H., Iri, M. & Murota, K. (1985). Voronoi diagram in the Laguerre geometry and its applications. *SIAM Journal on Computing*, *14*(1), 93–105. http://www.siam.org/journals/ojsa.php

Jiménez-Herrera, N., Barrios, G. K. P. & Tavares, L. M. (2018). Comparison of breakage models in DEM in simulating impact on particle beds. *Advanced Powder Technology*, *29*(3), 692–706. https://doi.org/10.1016/j.apt.2017.12.006

Laubscher, D. (1994). Cave mining - the state of the art. *The Journal of The South African Institute of Mining and Metallurgy*, *10*, 279–293.

Laubscher, D. H. (1994). Cave mining-the state of the art. *The Journal of South African Institute of Mining and Metallurgy*, 279–293.

Pierce, M., Weatherley, D. and Kojovic, T. (2010). A hybrid methodology for secondary fragmentation prediction in cave mines. Caving 2010, 567–581. https://doi.org/10.36487/acg_rep/1002_39_weatherley-pierce

Rumpf, H. (1973). Physical Aspects of Comminution and New Formulation of a Law of Comminution. *Powder Technology*, *7*, 145–159.

Shi, F. and Kojovic, T. (2007). Validation of a model for impact breakage incorporating particle size effect. *International Journal of Mineral Processing*, *82*(3), 156–163. https://doi.org/10.1016/j.minpro.2006.09.006

Veltin, K., Elmo, D. and Rogers, S. (2021). A Hybrid FEM/DEM Approach to Estimating Rock Block Breakage due to Gravity Free-Fall. IOP Conference Series: Earth and Environmental Science, 833(1). https://doi.org/10.1088/1755-1315/833/1/012098

Vogel, L. and Peukert, W. (2004). Determination of material properties relevant to grinding by practicable labscale milling tests. *International Journal of Mineral Processing*, *74*(S), 329–338. https://doi.org/10.1016/j.minpro.2004.07.018

Weibull, W. (1951). A Statistical Distribution Function of Wide Applicability. *Journal of Applied Mechanics*. https://hal.archives-ouvertes.fr/hal-03112318